

Low-Field Simulation and Minimum Field Strength Requirements

Ziyue Wu¹, Weiyi Chen¹, and Krishna S. Nayak¹
¹University of Southern California, Los Angeles, CA

PURPOSE: Low-field MRI systems are generally less expensive, and in some settings can provide equivalent diagnostic performance [1]. Our goal is to provide a simulation tool for determining the minimum field strength requirements for MRI methods, including novel data sampling and reconstruction techniques. Developers can test the potential applicability of their techniques at lower B_0 field strengths when higher-field experiments have been performed.

SOFTWARE DESCRIPTION: To simulate low-field raw data from data acquired at higher field, we make five modeling assumptions: (1) *Body noise dominance.* This can be achieved at 4 MHz or above in system sizes compatible with human extremities [2,3], suggesting the feasibility of most human MRI scans with body noise dominance at 0.1T or above. (2) *Consistent B_1^+ / B_1^- field.* RF transmit homogeneity is expected to improve at lower field strength, therefore this represents a worst case scenario. Receiver coils are assumed to have the same geometry and relative noise covariance at different field strengths. (3) *Consistent B_0 homogeneity.* We assume the same ppm off-resonance at different field strengths. (4) *Proton density weighting or single species dominance.* We use a single global relaxation correction function to account for the signal change at different B_0 . (5) *Steady state acquisition.*

The process for simulating low-field data is illustrated in **Fig. 1**. The acquired high-field k-space data is: $y_h = s_h + n_h$ where s_h and n_h are pure signal and noise respectively. n_h is bivariate and normally distributed: $Re\{n_h\} \sim N(0, \Sigma)$, $Im\{n_h\} \sim N(0, \Sigma)$ where $\Sigma \in \mathbb{R}^{k \times k}$ is the noise covariance matrix for a k-channel receiver coil and is measured by data acquisition with RF turned off. Thermal noise variance is proportional to B_0^2 and readout bandwidth BW. Therefore, the simulated noise \hat{n}_l at low field is: $Re\{\hat{n}_l\} \sim N(0, a^2 b \Sigma)$, $Im\{\hat{n}_l\} \sim N(0, a^2 b \Sigma)$ where $a = B_{0,l}/B_{0,h}$, $b = BW_l/BW_h$. The k-space signal at low field is modeled as: $\hat{s}_l = a^2 f s_h$ where f represents the signal change due to different relaxation as a function of B_0 . This is computed based on the pulse sequence parameters and the dominant species' relaxation times. Given f , the simulated low field k-space data is: $\hat{y}_l = \hat{s}_l + \hat{n}_l = a^2 f s_h + \hat{n}_l = a^2 f y_h + \hat{n}_{add}$, where $Re\{\hat{n}_{add}\} \& Im\{\hat{n}_{add}\} \sim N(0, (a^2 b - a^4 f^2) \Sigma)$.

Phantom studies were performed to validate the model above by comparing SNR at 1.5T/3T between the actual measurements and predictions from a 7T acquisitions. Modeling error was less than 8%. MATLAB source code is available: <http://mrel.usc.edu/share.html>.

EXAMPLE APPLICATION: Consider liver proton density fat fraction (PDFF) measurement using IDEAL SPGR (Acquisition: $B_0=3T$, TE 2.2/3.1/4.0ms, TR 9ms, flip angle 3° , BW 62.5KHz). $f = \frac{(1-E_{1,l})\sin\theta_l}{1-E_{1,l}\cos\theta_l} / \frac{(1-E_{1,h})\sin\theta_h}{1-E_{1,h}\cos\theta_h} e^{-(TE_l-TE_h)/T_2} e^{-c\gamma\Delta B_{ppm}(B_{0,l}TE_l-B_{0,h}TE_h)}$ (1) where $E_1 = \exp(-TR/T_1)$, c is a constant and ΔB_{ppm} is the ppm field inhomogeneity. To achieve the same phase shift between fat and water, the product of B_0 and TE needs to remain the same. Therefore simulated TE 's were set to be $(B_{0,h}/B_{0,l})$ times longer when simulated at low fields. Bandwidths were also set to $(B_{0,h}/B_{0,l})$ times shorter, enabled by longer TE 's. Given the small flip angle, (1) is reduced to $f \approx \exp[-(TE_l - TE_h)/T_2]$, with liver T2 being 42ms [4]. **Fig. 2** compares fat-water separated images and fat fractions for a single axial slice at different simulated field strengths. Images were reconstructed using the ISMRM fat-water toolbox [5,6]. PDFF for a manually defined region of interest (ROI) was computed from fifty independent simulations at each B_0 . PDFF precision (standard deviation) is worse as B_0 goes down. PDFF accuracy (mean) deviates from truth significantly at 0.1T, a result of dominant noise biasing estimated PDFF towards 50%. Although the accuracy and precision needed for a clinical liver fat biomarker is unknown [7], once determined, this analysis would facilitate determination of the required minimum B_0 . For example, if the accuracy and precision needed are both less than 2%, it suggests $B_0 = 0.3$ T would be sufficient.

DISCUSSION: Many new MR data sampling and reconstruction methods are developed and validated on state-of-the-art high-field instruments. It is informative to determine the potential to apply these techniques on more affordable low-field systems. Besides cost-efficiency, low-field MRI also has other attractive properties including reduced acoustic noise and SAR, safer for metal implants, more uniform RF transmission, and less off-resonance. With the help of advanced sampling and reconstruction techniques, many applications that were previously prohibited at low fields may become feasible now. More details can be found in [8].

REFERENCES: [1] Rutt et al., JMRI 1996(6):57-62. [2] Chronik et al., ISMRM 2002, p58 [3] Grafendorfer et al., ISMRM 2006, p2613. [4] Nishimura, Principles of MRI, 1996. [5] Hernando et al., MRM 2010(63):79-19. [6] Hu et al., MRM 2012(68):378-88. [7] Reeder et al., JMRI 2011(34):729-49. [8] USC SIPI technical report #417 (<http://sipi.usc.edu/reports/>)

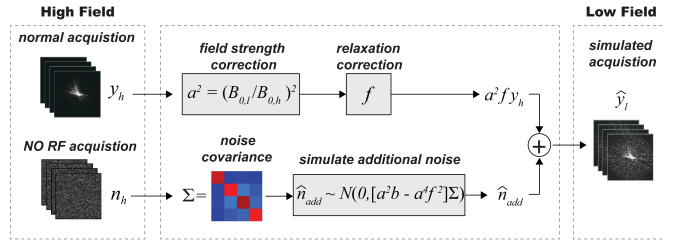


Figure 1. Simulation of low-field multi-coil k-space data. High-field k-space data y_h and pure noise n_h are acquired and serve as inputs. y_h is then scaled to account for signal change at different field strengths. Additional noise \hat{n}_{add} is added to compensate for the different noise levels.

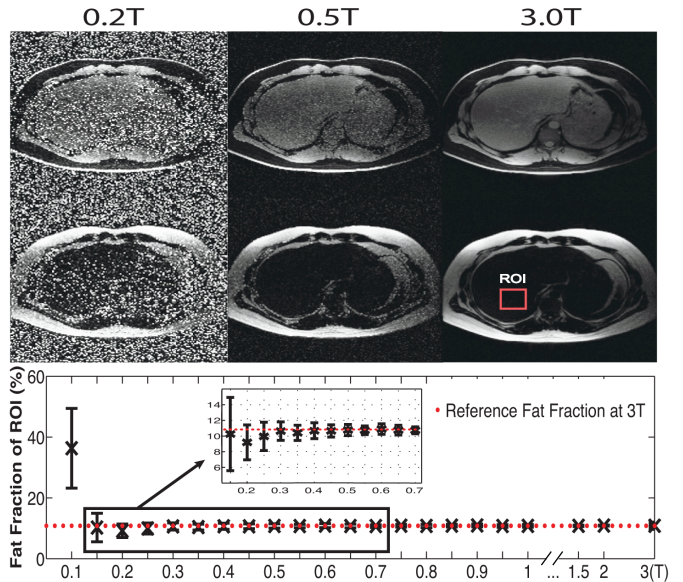


Figure 2. Top: Fat-water separated images. Bottom: The mean and standard deviation of fat fraction in the ROI at different field strengths. Fifty independent simulations were performed at each field strength.